Influence of CT-based attenuation correction in assessment of left and right ventricular functions with count-based gated blood-pool SPECT

Louis Sibille, MD, Fayçal Ben Bouallegue, PhD, Aurélie Bourdon, MD, and Denis Mariano-Goulart, PhD

Objective. **Influence of CT-based attenuation correction (CT-AC) in assessment of left and right ventricular functions with count-based gated blood-pool SPECT (GBPS) was evaluated in a mixed population.**

Methods. **Thirty-two patients (81% male; mean age 56 ± 12) referred for various symptoms or heart diseases were prospectively included. Data from 32 GBPS acquisitions were reconstructed using an iterative algorithm with (IRAC) and without (IRNC) CT-AC and analyzed using previously described segmentation software based on the watershed algorithm. LV and RV EF and volumes were assessed with and without CT-AC and compared.**

Results. **EF and volumes were correlated ($P < .001$ for all parameters with $r = 0.97$ for LV and RV EF; $r = 0.96$ for LV EDV; $r = 0.98$ for LV ESV; $r = 0.96$ for RV EDV and ESV). The mean values using IRAC and IRNC were different for all parameters with lower EF (respectively, 49% ± 19% vs 51 %± 18%; $P = .002$ for LV EF and 50% ± 14% vs 54%±15%; $P < .001$ for RV EF) and higher volumes (respectively, 142 ± 41 mL vs 133 ± 40 mL; $P < .001$ and 79 ± 45 mL vs 71 ± 42 mL; $P < .001$ for LV EDV and ESV; 91 ± 32 mL vs 86 ± 31 mL; $P = .003$ and 48 ± 28 mL vs 43 ± 26 mL; $P < .001$ for RV EDV and ESV). Limits of agreement were −11% to 6% and −11% to 4% for LV and RV EF. We found wider limits of agreement for LV volumes (−13 to 32 mL for EDV and −10 to 27 mL for ESV) than for RV volumes (−13 to 23 mL for EDV and −9 to 20 mL for ESV). Taking into account all volumes, we found a trend with a significant positive correlation between means and differences in volumes assessed with and without CT-AC.**

Conclusion. **Assessment of both left and right ventricular functions by count-based GBPS with CT-AC showed higher volumes and lower EF. Differences were slight, especially for the range of normal to subnormal ventricular volumes. (J Nucl Cardiol 2011)**

Key Words: Attenuation correction • gated blood-pool imaging • gated SPECT • Ventricular function

INTRODUCTION

Accurate quantification of ventricular function and volumes is important in the management of patients with cardiovascular disease. In patients with coronary artery disease, left ventricular (LV) ejection fraction (EF) at rest or stress, end-diastolic volume (EDV), and end-systolic volume (ESV) are strong independent predictors of cardiovascular morbidity and death.[1,2] Even patients without prior myocardial infarction or valvular disease are at high risk of congestive heart failure and death when only a mild impairment in LV EF is present.[3] Right ventricular (RV) EF is also a very important parameter, as, independently of pulmonary hypertension, it improves the accuracy of the prognostic stratification of patients with heart failure.[4]

Count-based gated blood-pool SPECT (GBPS) is a technically simple and widely available method that is independent of geometry. Thus, it may permit

From the Department of Nuclear Medicine, CHRU Lapeyronie, Montpellier, France.

Received for publication Mar 14, 2011; final revision accepted May 23, 2011.

Reprint requests: Louis Sibille, Department of Nuclear Medicine, CHRU Lapeyronie, 371 Av. du Doyen Gaston Giraud, 34295 Montpellier, France; *louis.sibille@gmail.com*.

1071-3581/$34.00

Copyright © 2011 American Society of Nuclear Cardiology.

doi:10.1007/s12350-011-9407-7

Published online: 07 June 2011

simultaneous assessment at equilibrium of the LV and RV parameters.[5-8] Regional ventricular function measurements like local EF or local times of end-systole are also available with this technique.[9-12] However, as for all nuclear medicine procedures, soft-tissue attenuation is a technical limitation when assessing tracer distribution, even with tomographic data and especially when only a 180° projection set is used.[13,14] The half-value layer of a single photon-emitting isotope like ^{99m}Tc (140 keV) is equal to approximately 4 cm in soft tissue.[15] This illustrates the essential impact of attenuation caused by photoelectric absorption and Compton scattering. For a given photon energy, attenuation coefficients can be determined, provided that the densities encountered by a gamma ray along a line of response are known. Therefore, SPECT attenuation correction (AC) is possible if acquisition of a density map is acquired together with the SPECT data.[16,17]

In the early 2000s, hybrid SPECT/CT systems consisting of multidetector SPECT coupled with conventional CT systems were commercially introduced.[18-20] CT provides two distinct advantages compared with the sealed sources that were previously used. It provides a significantly higher quality of attenuation measurement as a result of the greater photon flux and corresponding higher spatial resolution. Also, CT-based studies are performed sequentially and the very high flux dominates the count rates from ^{99m}Tc in the x-ray windows and crossover (downscatter artifacts) is thus negligible.

CT can be acquired in a relatively short time compared with SPECT, thus reducing the possibility of patient motion during the transmission data acquisition and between SPECT and CT acquisitions.[15,17] However, cardiac CT acquisitions with hybrid SPECT/CT systems are not gated and thus CT provides an average attenuation map for cardiac structures. In spite of this limitation, it has been proven that CT-AC can be useful for interpreting perfusion[15] and functional[21] data from gated myocardial perfusion imaging.

Count-based GBPS techniques use count rates to derive ventricular ejection fractions and volumes.[8] Therefore, these methods are likely to be more impacted by attenuation than edge detection, iterative thresholding, or surface gradient methods. There is a dearth of outcome studies dedicated to the evaluation of the clinical relevance of AC data for GBPS.[14] In this study, we investigated the influence of CT-AC in the assessment of left and right ventricular ejection fractions and volumes with GBPS.

MATERIALS AND METHODS

Patients

Thirty-two consecutive patients [aged 56 ± 12 years (range 30-78 years); 81% male; BMI 26 ± 6 kg/m^2] were prospectively included in the study. Eight (25%) patients had implanted cardiac devices. All patients had clinical indications for isotopic evaluation of EF and volumes, either to diagnose cardiac disease or as follow-up. Reasons for referral were coronary artery disease (n = 16), arrhythmogenic right ventricular dysplasia (n = 4), pulmonary hypertension (n = 2), evaluation of right ventricular parameters before cardiac assistance (n = 2), nonischemic dilated cardiomyopathy (n = 7), and chemotherapy-induced cardiac toxicity (n = 1). All subjects were prospectively recruited from inpatient and outpatient populations at the Montpellier University Hospital between August 6, 2009, and June 14, 2010. All patients gave their informed consent prior to inclusion in the study.

GBPS Data Acquisition

Patients were injected with 740-925 MBq (20-25 mCi) of in vitro labeled erythrocyte solution. They were in supine position with arms kept outside the field of view. Data were acquired on a hybrid SPECT-CT dual-head γ-camera (Infinia Hawkeye 4; GE Healthcare, Chalfont St. Giles, UK) in a 90° configuration with low-energy high-resolution parallel-hole collimators. Tomographic gated blood-pool scintigraphy was performed with the following acquisition parameters: 6° per step (15 steps over 90° per head) for 180° according to the American and European guidelines,[22,23] 40-s acquisition per step, 10% R-R interval acceptance window, 8 gated intervals, and 64 × 64 (pixel size: 5.9 mm).

Low-dose CT scan was acquired for attenuation correction using the following parameters: 140 kV, 2.5 mAs, 2.6 revolutions per minute for gantry rotation speeds, 256 × 256 (pixel size: 1.47 mm), and 6-mm slice thicknesses.[20,24] With these acquisition parameters, the examination time was 18 minutes (10 minutes for SPECT acquisition and 8 minutes for CT acquisition) for patients with regular pacing.

GBPS Processing

All acquisitions were reconstructed two times on a Xeleris workstation (GE Healthcare, Chalfont St. Giles, UK) with 16 transverse slices for each time frame using an ordered subsets-expectation maximization algorithm (2 iterations, 10 subsets, and a Butterworth post-processing filter: frequency 0.25; order 10) with (iterative reconstruction attenuation corrected, IRAC) and without (iterative reconstruction non-corrected, IRNC) CT-AC. AC map generation was performed on the Xeleris workstation (GE Healthcare, Chalfont St. Giles, UK). Matrix change was necessary to decrease the resolution of the CT data to match that of SPECT.[16] The accuracy of the registration between SPECT and CT data was verified using currently available attenuation correction quality control (ACQC) software provided by GE Healthcare systems. All registrations were visually validated before final image reconstruction.[25] The emission data underwent compensation for scatter using the Jaszczak method.[26] Transverse slices were reoriented into the usual cardiac axis and processed with in-house semiautomatic GBPS software based on a watershed segmentation algorithm (Tompool®: freely available on the net at

http://www.scinti.etud.univ-montp1.fr). In order to identify each segmented structure as belonging to the LV, the RV or the vascular structure behind the valve plane, septal, atrioventricular and pulmonary infundibulum planes were defined beforehand manually by one senior nuclear medicine physician with special training in cardiology. Segmentation obtained for IRNC data was automatically and exactly applied to IRAC data to nullify the intraoperator variability.

The previously described and validated Tompool® algorithm[5,7,9,27] was slightly modified and adapted to run on standard desktop personal computers running under Windows operating systems (Microsoft Corp., Redmond, WA). Iterative thinnings that were used to produce a skeleton by influence zones[5] were replaced by a full 3D immersion approach taking adjacent slices into consideration. This approach produced less over-segmentation of the ventricular cavities. In order to identify each segmented structure as belonging to the LV, the RV or the vascular structure behind the valve plane, septal, atrioventricular and pulmonary infundibulum planes were defined beforehand. These improvements led to a fully automatic algorithm, except for the precise location of the three aforementioned planes. Time-activity curves were generated using deformation of a reference curve, as described by Caderas De Kerleau et al.[10]

As described in previous published works, right or left ventricular ejection fractions, EF, and ventricular volumes, V, were calculated as:

$$\mathrm{EF} = \frac{C_{\mathrm{ED}} - C_{\mathrm{ES}}}{C_{\mathrm{ED}}} \quad \text{and} \quad V = \frac{C}{C_{\max}} \cdot V^{\mathrm{voxel}}$$

where C, C_{ED}, and C_{ES} are the total counts in a given ventricle at any time interval, at end diastole and at end systole, respectively; $C_{\max}$ is the maximal count in a voxel belonging to a ventricle; and V^{voxel} is the volume of a voxel.

Statistics

Statistical analysis was performed with commercially available software (SPSS for Windows, version 13.0; SPSS Inc., Chicago, IL; and GraphPad Prism for Windows, version 5, GraphPad Software Inc., La Jolla, CA). The mean ± standard deviation (SD) characterizes the distributions of the parameters for the data. Continuous data were compared with a paired Student's t test or a paired Wilcoxon test, as appropriate. Correlation between continuous variables was determined using linear regression and Spearman's rank order correlation coefficient. Bland-Altman analyses of measurement differences plotted versus mean values were used to assess biases (mean difference), trends, and 95% limits of agreement.[28] For all statistical testing, a two-tailed P value of less than .05 was considered statistically significant.

RESULTS

GBPS was performed successfully in all patients and no complications occurred. The mean heart rate and systolic/diastolic arterial pressure during GBPS acquisitions were 65 ± 12 bpm and 121 ± 19/69±11 mm Hg. All emission and transmission data were of sufficient quality and suitable for analysis. IRNC and IRAC algorithms were run for GBPS data for all 32 acquisitions. Calculations of RV and LV EF and volumes using Tompool® took less than 1 minute per reconstructed datum. The main results are presented in Table 1.

Ejection Fraction

LV EF assessed with IRNC and IRAC were correlated [$r = 0.97$; $P < .001$; standard error of estimate (SEE) = 4.24%] (Figure 1). The mean LV EF values for IRNC and IRAC were different (respectively, 51% ± 18% and 49% ± 19%; $P = .002$). Figure 1 shows a Bland-Altman plot of the LV EF measurements by IRNC and IRAC.

The results of the Bland-Altman analysis are summarized in Table 2, showing for EF a mean difference of −2.31% and 95% limits of agreement of −10.83% to 6.20%.

RV EF assessed with IRNC and IRAC were correlated ($r = 0.97$; $P < .001$; SEE = 3.76%) (Figure 1). The mean RV EF values for IRNC and IRAC were different (respectively, 54% ± 15% and 50% ± 14%; $P < .001$). Figure 1 shows a Bland-Altman plot of the RV EF measurements by IRNC and IRAC. The results of the Bland-Altman analysis are summarized in

Table 1. Left and right ventricular parameters without (IRNC) and with (IRAC) CT-based attenuation correction

	Left ventricle			Right ventricle		
	EF	EDV	ESV	EF	EDV	ESV
IRNC	51 ± 18	133 ± 40	71 ± 42	54 ± 15	86 ± 31	43 ± 26
IRAC	49 ± 19	142 ± 41	79 ± 45	50 ± 14	91 ± 32	48 ± 28

EDV, End-diastolic volume; *ESV*, end-systolic volume; *EF*, ejection fraction; *IRNC/IRAC*, iterative reconstruction non-corrected/attenuation corrected.

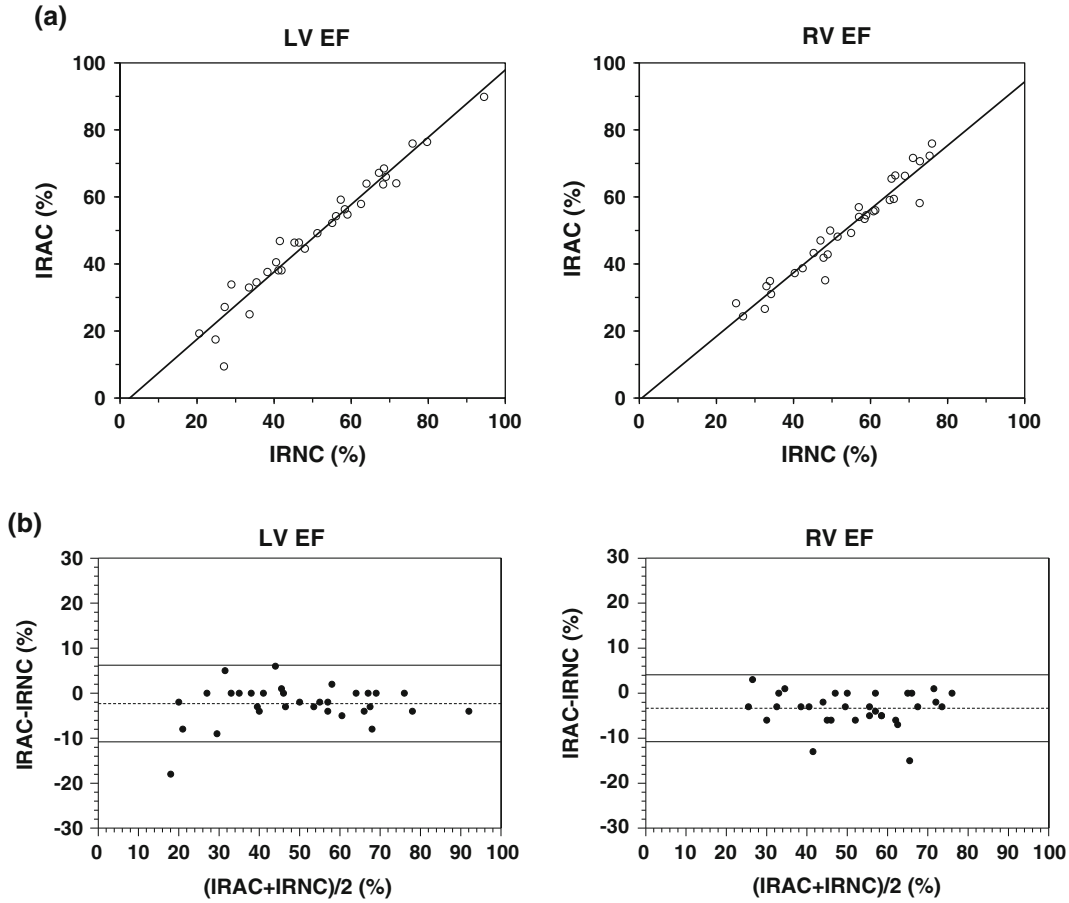

Figure 1. Left and right ventricular ejection fractions (LV and RV EF) using IRNC and IRAC algorithms: **A** Regression curves, $LVEF_{IRAC} = 1.00\ LVEF_{IRNC} - 2.55$; $R^2 = 0.95$; SEE = 4.24; $r = 0.97$; $P < .001$. $RVEF_{IRAC} = 0.95\ RVEF_{IRNC} - 0.60$; $R^2 = 0.93$; SEE = 3.76; $r = 0.97$; $P < .001$. **B** Bland-Altman plots, *horizontal lines* indicate the mean difference and 95% limits of agreement (95% LA).

Table 2, showing for EF a mean difference of −3.34% and 95% limits of agreement of −10.79% to 4.10%.

Volumes

LV EDV and ESV assessed with IRNC and IRAC were correlated (respectively, $r = 0.96$; $P < .001$; SEE = 11.82 mL and $r = 0.98$; $P < .001$; SEE = 9.25 mL) (Figure 2). The mean LV EDV and ESV values for IRNC and IRAC were different (respectively, 133 ± 40; 142 ± 41 mL; $P < .001$ and 71 ± 42; 79 ± 45 mL; $P < .001$). Figure 2 shows a Bland-Altman plot of LV EDV and ESV measurements by IRNC and IRAC. The results of the Bland-Altman analysis are summarized in Table 3, showing for EDV a mean difference of 9.47 mL and 95% limits of agreement of −13.36 to 32.30 mL and for ESV a mean difference of 8.53 mL and 95% limits of agreements of −10.34 to 27.40 mL.

RV EDV and ESV assessed with IRNC and IRAC were correlated (respectively, $r = 0.96$; $P < .001$; SEE = 9.44 mL and $r = 0.96$; $P < .001$; SEE = 7.03 mL) (Figure 2). The mean RV EDV and ESV values for IRNC and IRAC were different (respectively, 86 ± 31 and 91 ± 32 mL; $P = .003$ and 43 ± 26 and 48 ± 28 mL; $P < .001$). Figure 2 shows a Bland-Altman plot of RV EDV and ESV measurements by IRNC and IRAC. The results of the Bland-Altman analysis are summarized in Table 3, showing for EDV a mean difference of 5.16 mL and 95% limits of agreement of −12.98 to 23.29 mL and for ESV a mean difference of 5.47 mL and 95% limits of agreement of −8.59 to 19.52 mL.

Figure 3 shows a Bland-Altman plot of all left and right ventricular volume measurements by IRNC and IRAC. The results of the Bland-Altman analysis are summarized in Table 3, showing a mean difference of 7.16 mL and 95% limits of agreement of −11.72 to

Table 2. Comparisons between left and right ventricular ejection fractions without (IRNC) and with (IRAC) CT-based attenuation correction

	LVEF	RVEF
Correlation		
r	0.97	0.97
P	<.001	<.001
Regression line		
Slope	1.00 ± 0.04	0.95 ± 0.05
y_0	−2.55 ± 2.27	−0.60 ± 2.55
Difference (IRAC − IRNC)		
Mean ± SD	−2.31 ± 4.34	−3.34 ± 3.80
95% LA	[−10.83; 6.20]	[−10.79; 4.10]
SEM	0.77	0.67
95% CI	[−3.84; −0.78]	[−4.68; −2.00]
Bias	Yes	Yes

95% *LA*, 95% limits of agreement; *SEM*, standard error of the mean difference; 95% *CI*, 95% confidence interval.

26.03 mL. A trend with a significant correlation ($r = 0.26$; $P = .003$; SEE = 9.37 mL) is illustrated by the regression line ($y_0 = 4.52$; slope = 0.04).

DISCUSSION

CT-AC for SPECT has been well established, but there is a lack of study on influence of CT-AC in the assessment of LV and RV function with GBPS. In a short communication, Seierstad et al[14] did not report SPECT studies on patients, but instead the attenuation of photons was simulated numerically. Our investigation demonstrated that both LV and RV volumes were slightly higher when CT-AC was performed. Our results corroborate earlier studies made on a cardiac torso phantom.[13,14] Pretorius et al[13] found that LV and RV parameters were more accurately assessed when using one iteration of Chang's attenuation correction method. They concluded that this method was able to reduce the distortion of counts. Because of the heterogeneous density of the thorax and chest wall, the CT-based method should be even more precise. Moreover, it performs a patient-specific attenuation correction.

A precedent study showed that in spite of their totally different approaches, the volume measurements by non-CT-AC GBPS and cardiac magnetic resonance (CMR) were in quite close agreement.[8] However, lower volumes were found with non-CT-AC GBPS for the LV and RV volumes, with respective mean differences of 36 ± 2 mL for EDV and 19 ± 2 mL for ESV. The inclusion of papillary muscles and trabeculations in performing CMR cavity drawings significantly affects quantifications of LV volume and can partially explain these differences.[29] In this study, we found a significant increase in LV and RV volumes when using CT-AC, with respective mean differences of 9(+7%) and 5(+6%) mL for EDV and 9(+12%) and 5(+13%) mL for ESV, thereby suggesting that photon attenuation may also partly explain the differences between GBPS and CMR results. One part of the origins of this attenuation is the blood pool itself and so-called self-attenuation. However, the EDV and ESV mean differences were equal for both ventricles, suggesting that for this range of volumes the influence of self-attenuation is poor. It should be greater in patients with dilated cardiomyopathy, and in fact we found a trend with a significant correlation on the Bland-Altman plot of all left and right volumes using the IRNC and IRAC algorithms (Figure 3). The increasing volume differences between IRNC and IRAC suggested that large volumes were more influenced by radiation attenuation, probably because of prominent self-attenuation. The differences between the IRNC and IRAC volumes were greater for the LV than for the RV. Several factors would explain this finding, such as the higher LV volumes in the study population, the position of the heart within the chest cavity, and the shape and structure of the LV.

A simple differential calculation showed that the decrease in EF with AC was equivalent to a relative increase in end-systolic activity greater than that at end-diastole. As volumes are derived from systolic and diastolic counts through a linear relation, this implies that volumes were also relatively more increased by AC at end-systole than at end-diastole. We suggest the following 2-point hypothesis. First, because of the location and orientation of the heart in the chest, voxels located in the basal and mid-central areas of the ventricular cavities are the most influenced by attenuation when using 180° acquisition.[15] The activity of these voxels should not change much during the cardiac cycle, given the deformations of the ventricular cavities. These voxels are kept full of blood during the entire cardiac cycle and correspond to the ESV. The second point concerns the potential overcorrection of the systole data. Because of the slow-acquisition CT scanner used in this study, the CT images used for attenuation correction were blurred, not only by the change in matrix necessary for adaptation to the SPECT images, but also by the physiologic motion of the heart and lungs. This is actually an advantage, leading to a good match in fused images, but we can question whether the single attenuation map that was generated would not be more representative of the diastolic phase, thus leading to an overcorrection of the systolic phase data.

The limitations of this study include a relatively small sample size and an inhomogeneous study

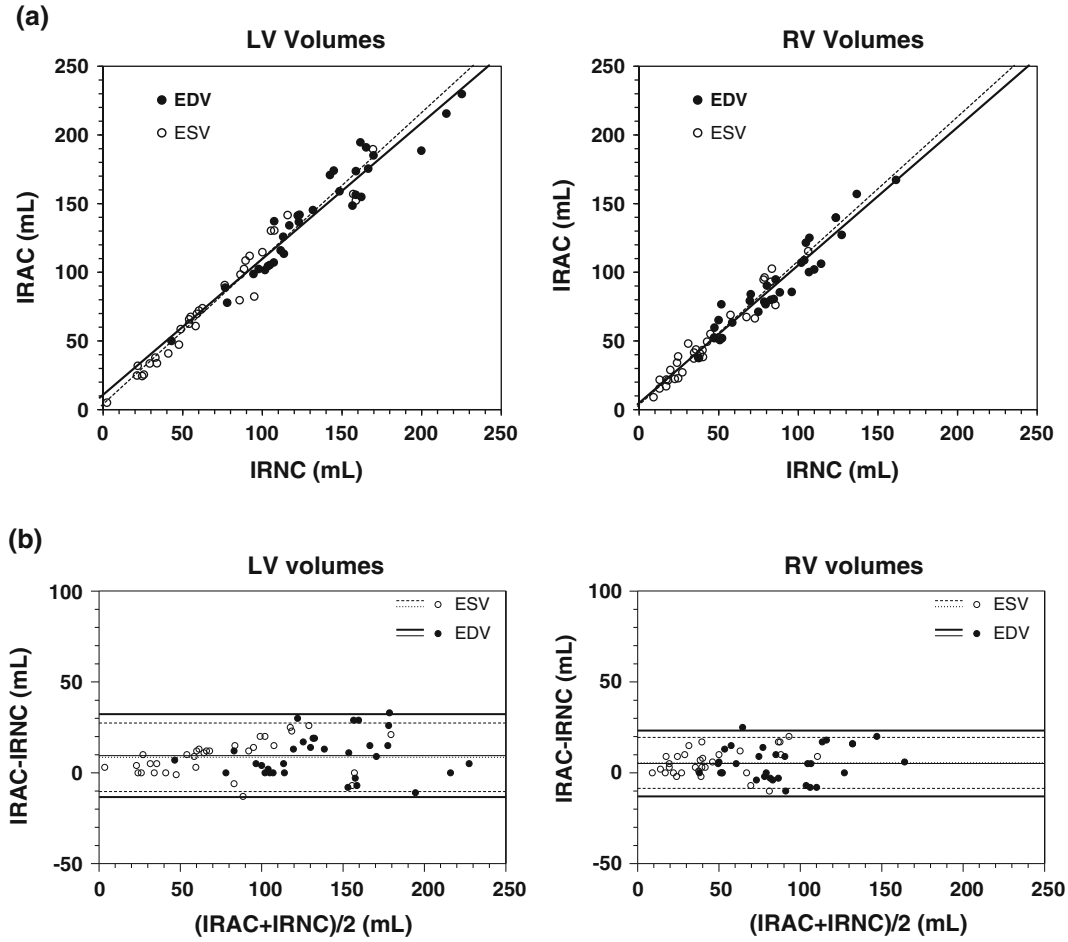

Figure 2. Left and right ventricular end-diastolic (EDV) and end-systolic (ESV) volumes using IRNC and IRAC algorithms: **A** Left ventricular volume regression curves, $EDV_{IRAC} = 0.99\ EDV_{IRNC} + 10.85$; $R^2 = 0.92$; SEE = 11.82; $r = 0.96$; $P < .001$. $ESV_{IRAC} = 1.06\ ESV_{IRNC} + 4.10$; $R^2 = 0.96$; SEE = 9.25; $r = 0.98$; $P < .001$. Right ventricular volume regression curves, $EDV_{IRAC} = 1.00\ EDV_{IRNC} + 4.87$; $R^2 = 0.92$; SEE = 9.44; $r = 0.96$; $P < .001$. $ESV_{IRAC} = 1.05\ EDV_{IRNC} + 3.46$; $R^2 = 0.94$; SEE = 7.03; $r = 0.96$; $P < .001$. **B** Bland-Altman plots, *horizontal lines* indicate the mean difference and 95% limits of agreement (95% LA).

population with few women. We could not study attenuation effect in specific subpopulation such as obese patients or patients with cardiac hypertrophy. Influence of CT-AC may be more prominent in patients with BMI greater than 30 kg/m^2. Nevertheless, our study demonstrated that both left and right ventricular volumes were slightly lower when CT-AC was not performed. Volume differences were relatively constant and low for volumes not greater than 100 mL. For greater volumes, the differences increased slowly, probably because of prominent self-attenuation. The decreases in EF were probably due to an overcorrection of end-systolic counts. All in all, the differences introduced by AC in the EF and volume estimations remained small for the range of normal patient values and should remain of minor importance for most clinical studies. We decided not to use AC for our daily practice, given its above-mentioned limited influence and the low but real increase in patient radiation dose. Moreover, further study using a physical phantom and comparison with MRI are necessary to determine whether volumes and EF evaluations with AC are more accurate than those assessed without it. Impact on clinical management in specific population (obese) and specific cardiac diseases (dilated or hypertrophic cardiomyopathy) has to be evaluated.

CONCLUSION

Assessment of both LV and RV function by count-based GBPS with CT-AC showed higher volumes and

Table 3. Comparisons between left and right ventricular volumes without (IRNC) and with (IRAC) CT-based attenuation correction

	LV EDV	LV ESV	RV EDV	RV ESV	All volumes
Correlation					
r	0.96	0.98	0.96	0.96	0.98
P	<.001	<.001	<.001	<.001	<.001
Regression line					
Slope	0.99 ± 0.05	1.06 ± 0.04	1.00 ± 0.05	1.05 ± 0.05	1.03 ± 0.02
y_0	10.85 ± 7.30	4.10 ± 3.25	4.87 ± 5.03	3.46 ± 2.42	4.60 ± 1.68
Difference (IRAC − IRNC)					
Mean ± SD	9.47 ± 11.65	8.53 ± 9.63	5.16 ± 9.25	5.47 ± 7.17	7.16 ± 9.63
95% LA	[−13.36; 32.30]	[−10.34; 27.40]	[−12.98; 23.29]	[−8.59; 19.52]	[−11.72; 26.03]
SEM	1.67	1.70	1.63	1.27	1.27
95% CI	[6.12; 12.82]	[5.13; 11.93]	[1.90; 8.42]	[2.93; 8.01]	[4.62; 9.70]
Bias	Yes	Yes	Yes	Yes	Yes

95% *LA*, 95% limits of agreement; *SEM*, standard error of the mean difference; 95% *CI*, 95% confidence interval.

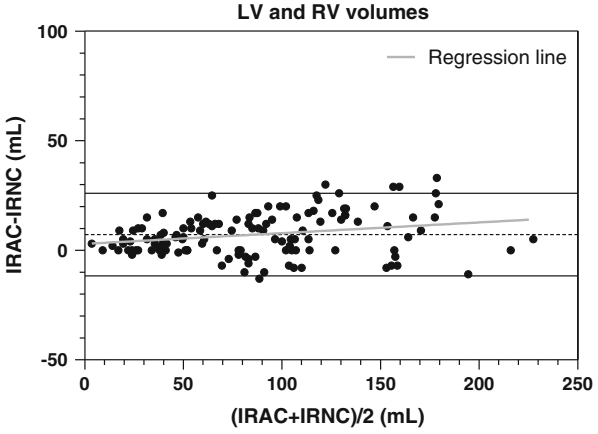

Fig. 3. All left and right ventricular volumes using IRNC and IRAC algorithms: Bland-Altman plots, *horizontal lines* indicate the mean difference and 95% limits of agreement (95% LA). Regression curve, $V_{IRAC} = 0.04\ V_{IRNC} + 4.52$; $R^2 = 0.04$; SEE = 9.37; $r = 0.26$; $P = .003$.

lower EF. All differences were slight, especially for the range of normal to subnormal ventricular volumes.

Acknowledgment

None.

Conflict of interest

The authors declare that they have no conflict of interest.

References

1. White HD, Norris RM, Brown MA, Brandt PW, Whitlock RM, Wild CJ. Left ventricular end-systolic volume as the major determinant of survival after recovery from myocardial infarction. Circulation 1987;76:44-51.
2. Sharir T, Germano G, Kavanagh PB, Lai S, Cohen I, Lewin HC, et al. Incremental prognostic value of post-stress left ventricular ejection fraction and volume by gated myocardial perfusion single photon emission computed tomography. Circulation 1999;100:1035-42.
3. Wang TJ, Evans JC, Benjamin EJ, Levy D, LeRoy EC, Vasan RS. Natural history of asymptomatic left ventricular systolic dysfunction in the community. Circulation 2003;108:977-82.
4. Ghio S, Gavazzi A, Campana C, Inserra C, Klersy C, Sebastiani R, et al. Independent and additive prognostic value of right ventricular systolic function and pulmonary artery pressure in patients with chronic heart failure. J Am Coll Cardiol 2001;37:183-8.
5. Mariano-Goulart D, Collet H, Kotzki PO, Zanca M, Rossi M. Semi-automatic segmentation of gated blood pool emission tomographic images by watersheds:application to the determination of right and left ejection fractions. Eur J Nucl Med 1998;25:1300-7.
6. Daou D, Harel F, Helal BO, Fourme T, Colin P, Lebtahi R, et al. Electrocardiographically gated blood-pool SPECT and left ventricular function: Comparative value of 3 methods for ejection fraction and volume estimation. J Nucl Med 2001;42:1043-9.
7. Mariano-Goulart D, Piot C, Boudousq V, Raczka F, Comte F, Eberle MC, et al. Routine measurements of left and right ventricular output by gated blood pool emission tomography in comparison with thermodilution measurements: A preliminary study. Eur J Nucl Med 2001;28:506-13.
8. Sibille L, Bouallegue FB, Bourdon A, Micheau A, Vernhet-Kovacsik H, Mariano-Goulart D. Comparative values of gated blood-pool SPECT and CMR for ejection fraction and volume estimation. Nucl Med Commun 2011;32:121-8.
9. Mariano-Goulart D, Dechaux L, Rouzet F, Barbotte E, Caderas de Kerleau C, Rossi M, et al. Diagnosis of diffuse and localized arrhythmogenic right ventricular dysplasia by gated blood-pool SPECT. J Nucl Med 2007;48:1416-23.
10. Caderas de Kerleau C, Ahronovitz E, Rossi M, Mariano-Goulart D. Automatic ventricular wall motion analysis by gated blood-pool emission tomography using deformations of an ideal time-activity curve. IEEE Trans Med Imaging 2004;23:485-91.
11. Nichols KJ, Van Tosh A, Wang Y, Palestro CJ, Reichek N. Validation of gated blood-pool SPECT regional left ventricular function measurements. J Nucl Med 2009;50:53-60.

12. Nichols KJ, Van Tosh A, De Bondt P, Bergmann SR, Palestro CJ, Reichek N. Normal limits of gated blood pool SPECT count-based regional cardiac function parameters. Int J Cardiovasc Imaging 2008;24:717-25.
13. Pretorius PH, Xia W, King MA, Tsui BM, Pan TS, Villegas BJ. Evaluation of right and left ventricular volume and ejection fraction using a mathematical cardiac torso phantom. J Nucl Med 1997;38:1528-35.
14. Seierstad T, Bogsrud T, Skretting A. Effects of photon attenuation on the determination of cardiac volumes from reconstructed counts in gated blood pool SPET. Eur J Nucl Med Mol Imaging 2004;31:399-402.
15. Bateman TM, Cullom SJ. Attenuation correction single-photon emission computed tomography myocardial perfusion imaging. Semin Nucl Med 2005;35:37-51.
16. Zaidi H, Hasegawa B. Determination of the attenuation map in emission tomography. J Nucl Med 2003;44:291-315.
17. Bailey DL. Transmission scanning in emission tomography. Eur J Nucl Med 1998;25:774-87.
18. Lang TF, Hasegawa BH, Liew SC, Brown JK, Blankespoor SC, Reilly SM, et al. Description of a prototype emission-transmission computed tomography imaging system. J Nucl Med 1992;33:1881-7.
19. Bocher M, Balan A, Krausz Y, Shrem Y, Lonn A, Wilk M, et al. Gamma camera-mounted anatomical X-ray tomography: Technology, system characteristics and first images. Eur J Nucl Med 2000;27:619-27.
20. Patton JA, Delbeke D, Sandler MP. Image fusion using an integrated, dual-head coincidence camera with X-ray tube-based attenuation maps. J Nucl Med 2000;41:1364-8.
21. Slart RH, Tio RA, Zeebregts CJ, Willemsen AT, Dierckx RA, De Sutter J. Attenuation corrected gated SPECT for the assessment of left ventricular ejection fraction and volumes. Ann Nucl Med 2008;22:171-6.
22. Hansen CL, Goldstein RA, Akinboboye OO, Berman DS, Botvinick EH, Churchwell KB, et al. Myocardial perfusion and function: Single photon emission computed tomography. J Nucl Cardiol 2007;14:e39-60.
23. Hesse B, Lindhardt TB, Acampa W, Anagnostopoulos C, Ballinger J, Bax JJ, et al. EANM/ESC guidelines for radionuclide imaging of cardiac function. Eur J Nucl Med Mol Imaging 2008;35:851-85.
24. Hamann M, Aldridge M, Dickson J, Endozo R, Lozhkin K, Hutton BF. Evaluation of a low-dose/slow-rotating SPECT-CT system. Phys Med Biol 2008;53:2495-508.
25. Tonge CM, Ellul G, Pandit M, Lawson RS, Shields RA, Arumugam P, et al. The value of registration correction in the attenuation correction of myocardial SPECT studies using low resolution computed tomography images. Nucl Med Commun 2006;27:843-52.
26. Jaszczak RJ, Floyd CE, Coleman RE. Scatter compensation techniques for SPECT. IEEE Trans Nucl Sci 1985;32:786-93.
27. Mariano-Goulart D, Caderas de Kerleau C, Rossi M. Automatic measurements of local ventricular parameters using Gated Blood-Pool Emission tomography. Médecine nucléaire 2005;29:115-30.
28. Bland JM, Altman DG. Statistical methods for assessing agreement between two methods of clinical measurement. Lancet 1986;1:307-10.
29. Papavassiliu T, Kuhl HP, Schroder M, Suselbeck T, Bondarenko O, Bohm CK, et al. Effect of endocardial trabeculae on left ventricular measurements and measurement reproducibility at cardiovascular MR imaging. Radiology 2005;236:57-64.